



HAL
open science

Cooling of Microprocessors Using Flow Boiling of CO in a Micro-Evaporator: Preliminary Analysis and Performance Comparison

Lixin Cheng, John R. Thome

► **To cite this version:**

Lixin Cheng, John R. Thome. Cooling of Microprocessors Using Flow Boiling of CO in a Micro-Evaporator: Preliminary Analysis and Performance Comparison. Applied Thermal Engineering, 2009, 29 (11-12), pp.2426. 10.1016/j.applthermaleng.2008.12.019 . hal-00528080

HAL Id: hal-00528080

<https://hal.science/hal-00528080>

Submitted on 21 Oct 2010

HAL is a multi-disciplinary open access archive for the deposit and dissemination of scientific research documents, whether they are published or not. The documents may come from teaching and research institutions in France or abroad, or from public or private research centers.

L'archive ouverte pluridisciplinaire **HAL**, est destinée au dépôt et à la diffusion de documents scientifiques de niveau recherche, publiés ou non, émanant des établissements d'enseignement et de recherche français ou étrangers, des laboratoires publics ou privés.

Accepted Manuscript

Cooling of Microprocessors Using Flow Boiling of CO₂ in a Micro-Evaporator:
Preliminary Analysis and Performance Comparison

Lixin Cheng, John R. Thome

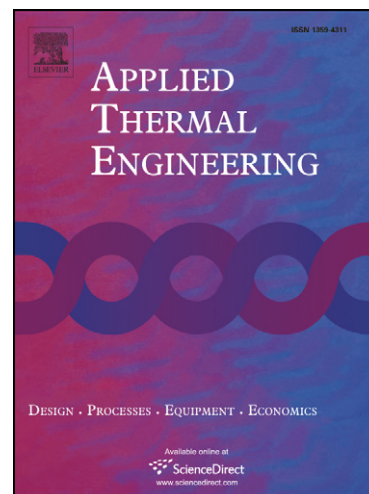
PII: S1359-4311(08)00485-7
DOI: [10.1016/j.applthermaleng.2008.12.019](https://doi.org/10.1016/j.applthermaleng.2008.12.019)
Reference: ATE 2690

To appear in: *Applied Thermal Engineering*

Received Date: 6 October 2008
Revised Date: 1 December 2008
Accepted Date: 14 December 2008

Please cite this article as: L. Cheng, J.R. Thome, Cooling of Microprocessors Using Flow Boiling of CO₂ in a Micro-Evaporator: Preliminary Analysis and Performance Comparison, *Applied Thermal Engineering* (2008), doi: [10.1016/j.applthermaleng.2008.12.019](https://doi.org/10.1016/j.applthermaleng.2008.12.019)

This is a PDF file of an unedited manuscript that has been accepted for publication. As a service to our customers we are providing this early version of the manuscript. The manuscript will undergo copyediting, typesetting, and review of the resulting proof before it is published in its final form. Please note that during the production process errors may be discovered which could affect the content, and all legal disclaimers that apply to the journal pertain.



Cooling of Microprocessors Using Flow Boiling of CO₂ in a Micro-Evaporator: Preliminary Analysis and Performance Comparison

Lixin Cheng^{a,b*}, John R. Thome^b

^a*School of Engineering, University of Aberdeen, King's College, Aberdeen, AB24 3FX, Scotland, the UK*

^b*Laboratory of Heat and Mass Transfer (LTCM), Faculty of Engineering (STI), École Polytechnique Fédérale de Lausanne (EPFL), Station 9, Lausanne, CH-1015, Switzerland*

Abstract

The flow pattern based flow boiling heat transfer and two-phase pressure drop models for CO₂, recently developed by Cheng et al. [1, 2], have been used to predict the thermal performance of CO₂ in a silicon multi-microchannel evaporator (67 parallel channels with a width of 0.223 mm, a height of 0.68 mm and a length of 20 mm) for cooling of a micro-processor. First, some simulation results of CO₂ flow boiling heat transfer and two-phase pressure drops in micro-scale channels are presented. The effects of channel diameter, mass flux, saturation temperature and heat flux on flow boiling heat transfer coefficients and two-phase pressure drops are next addressed. Then, simulations of the base temperatures of the silicon multi-microchannel evaporator using R236fa and CO₂ were performed for the following conditions: base heat fluxes from 20 to 100 W/cm², a mass flux of 987.6 kg/m²s and a saturation temperature of 25°C. These show that the base temperatures using CO₂ are much lower than those using R236fa. Compared to R236fa, CO₂ has much higher heat transfer coefficients and lower pressure drops in the multi-microchannel evaporator. However, the operation pressure of CO₂ is much higher than that of R236fa. Based on the analysis and comparison, CO₂ appears to be a promising coolant for microprocessors at low operating temperatures but also presents a great technological challenge like other new cooling technologies.

Keywords: CO₂; Flow boiling; Heat transfer; Evaporation; Two-phase flow; Pressure drop; Micro-Channel; Chips; Cooling; Micro-processor; Micro-evaporator.

* Corresponding author. Tel.: +41 21 693 5447; fax: +41 21 693 5960. *Email address:* lixincheng@hotmail.com (L. Cheng).

Nomenclature

A	[m ²]	Channel cross section area
D	[m]	Channel diameter
e	[m]	Thickness of channel base
G	[kg/m ² s]	Mass flux
g	[m/s ²]	Gravitational acceleration
H	[m]	Channel height
h	[W/m ² K]	Heat transfer coefficient
i_{LV}	[J/kg]	Latent heat of vaporization
k	[W/mK]	Thermal conductivity
L	[m]	Channel length
m	[1/m]	Parameter in Eq. (9)
N	[-]	Channel number
p	[Pa]	Pressure
q	[W/m ²]	Heat flux
T	[K]	Temperature
t	[m]	Channel wall thickness
W	[m]	Channel width
x	[-]	Vapor quality
z	[m]	Distance along flow direction in the channel

Greeks

Δp	[Pa]	Pressure drop
ΔT	[K]	Temperature difference
ε	[-]	Void fraction
η	[-]	Fin efficiency
μ	[Pas]	Viscosity
ρ	[kg/m ³]	Density

σ [N/m] Surface tension

Subscripts

a Acceleration
b Base
eq Equivalent
f Frictional
h Hydraulic
in Inlet
L Liquid
out Outlet
sat saturation
si Silicon
sub Subcooled
total total
V Vapor
W Wall
z At z distance

1. Introduction

Advances in micro-electronics technology continue to develop with surprisingly rapidity and the thermal energy density of electronic devices to be dissipated is becoming much higher. Therefore, it is essential to develop new high heat flux cooling technology to meet the challenging heat dissipation requirements [3-8].

With the rapid miniaturization of devices to nanoscale and microscale, the new technologies taking advantage of these advances are faced with very serious heat dissipation problems per unit volume (cooling CPUs and power electronics). The main issues in future trends for cooling of microprocessors are to dissipate footprint heat fluxes as high as 300 W/cm² or more while maintaining the chip safely below its maximum working temperature (less than 85°C) and providing a nearly uniform chip base temperature, the whole with a

minimal energy consumption. This means that conventional cooling technology, i.e. air cooling, will no longer be able to satisfy these heat duties. New solutions must be found to solve this problem. One possible solution is to use forced vaporization in micro-channels (multi-channels made in silicon or copper cooling elements attached to CPUs, or directly in the silicon chip itself) by making use of the high heat transfer performance of two-phase flows [3-15]. In this aspect, flow boiling of low pressure refrigerants in multi-channel evaporators is a promising technique. The recent experimental results of high heat flux flow boiling of two refrigerants R236fa and R245fa in silicon multi-microchannels by our laboratory have shown very good heat transfer behaviors [14, 15].

To further explore the use of environmentally friendly refrigerants for the cooling of micro-processors, the present paper presents analysis of cooling of microprocessors using flow boiling of CO₂ in a silicon multi-microchannel evaporator. CO₂ is a natural refrigerant and has been intensively investigated for automobile air-conditioning, refrigeration and heat pump systems over the past decade [1, 2, 16-20]. It has no ozone depletion potential (ODP = 0) and a negligible direct global warming potential (GWP = 1). For usual ambient air temperatures, the heat transfer process on the high pressure side of a CO₂ cycle is not a condensation process as in conventional systems but a supercritical gas cooling process [19, 20]. Hence, the conventional condenser is replaced by a gas cooler that rejects heat under variable temperature at high pressure. The heat transfer of supercritical CO₂ in the gas cooler is poorer than condensation heat transfer. To improve the performance of the CO₂ system, an internal heat exchanger is used to subcool the refrigerant between the gas cooler and the expansion device and to superheat the refrigerant in the suction line of the compressor. Furthermore, the compressor for the transcritical CO₂ cycle requires thicker walls to contain the high operating pressure, but since the volumetric capacity of the fluid is large, the compressor itself will actually be smaller than the refrigeration compressors for the same capacity using conventional refrigerants [19]. For the evaporation on the low pressure side, CO₂ evaporates at much higher pressure than other refrigerants. In this case, the physical and transport properties of CO₂ are quite different from those of conventional refrigerants at the same saturation temperatures. CO₂ has higher liquid and vapor thermal conductivities, a lower vapor-liquid density ratio (lower liquid and higher vapor densities), a very low surface tension, and a lower liquid-vapor viscosity ratio (lower liquid and higher vapor viscosities) than conventional refrigerants, thus flow boiling heat transfer, two-phase flow pattern and pressure drop characteristics are quite different from those of conventional low pressure refrigerants. Previous experimental studies have shown that CO₂ has higher flow boiling heat transfer coefficients and lower pressure drops than those of conventional refrigerants at the same saturation temperatures [1, 2, 16-18]. Thus,

use of CO₂ in a micro-channel evaporator has a great advantage over other refrigerants. In the present study, only the cooling performance of CO₂ in the micro-channel evaporator is focused on.

The available flow boiling heat transfer correlations developed for conventional low pressure refrigerants generally significantly underpredict the experimental data of CO₂. Therefore, new flow pattern based heat transfer and pressure drop models for CO₂ evaporation have been recently developed in our laboratory for use in the design of micro-channel evaporators in automobile air-conditioning systems [1, 2] and are improvements of our previous models [17-18]. These models accurately predicted heat transfer coefficients, flow patterns and pressure drops over a wide range of conditions, including tube diameters from 0.6 to 10.06 mm. Especially, these models predicted the heat transfer and pressure drops in both single and multi micro-channels.

In the present study, our recent models for CO₂ [1, 2] have been used to predict the thermal performance of CO₂ evaporation in a silicon multi-microchannel evaporator (67 parallel channels with a width of 0.223 mm, a height of 0.68 mm and a length of 20 mm). This geometry was chosen since we have recent test data for such a test section with a low pressure refrigerant R236fa [14]. First, some simulated results of CO₂ flow boiling heat transfer and two-phase pressure drops in micro-scale channels are presented for various conditions. The effects of channel diameter, mass flux, saturation temperature and heat flux on flow boiling heat transfer coefficients and two-phase pressure drops are analyzed. Then, simulations of base temperatures of the silicon multi-microchannel evaporator, comparing R236fa and CO₂ evaporation, have been performed for the following conditions: base heat fluxes $q_b = 20\text{-}100\text{ W/cm}^2$, mass flux $G = 987.6\text{ kg/m}^2\text{s}$ and saturation temperature $T_{sat} = 25^\circ\text{C}$.

2. Silicon Multi-Microchannel Evaporator

R236fa is chosen here for the comparison to CO₂ in a silicon multi-microchannel evaporator because an experimental study of high heat flux flow boiling of two refrigerants R236fa in the silicon multi-microchannel evaporator was recently conducted by our laboratory and the experimental results have shown very good heat transfer behaviors [14].

2.1. Geometry of Silicon Multi-Microchannel Evaporator

Figure 1 shows the schematic diagram of the silicon multi-microchannel heat sink investigated in the present paper. It consists of 67 microchannels. The dimensions of the microchannels are the same as those of Agostini et al. [14] and are given in Table 1, where the hydraulic diameter and equivalent diameter are defined as

$$D_h = \frac{2WH}{W+H} \quad (1)$$

$$D_{eq} = \sqrt{\frac{4A}{\pi}} = \sqrt{\frac{4WH}{\pi}} \quad (2)$$

The physical model is described as follows: (i) the bottom of the heat sink is uniformly heated by electric heating at a base heat flux q_b , (ii) the top of the heat sink is adiabatic, and (iii) the coolant (CO₂ or R236fa) flows in the silicon multi-microchannel evaporator without inlet subcooling, $\Delta T_{sub} = 0$ K; (iv) flow is uniformly distributed in the micro-channels. With these conditions, the base temperature T_b will be simulated using CO₂ and R236fa evaporation in the silicon microchannel evaporator at some operational conditions and the simulated results will be compared.

2.2. Physical Properties of R236fa and CO₂

Table 1 shows a comparison of selected physical properties of R236fa and CO₂ at a saturation temperature $T_{sat} = 15^\circ\text{C}$, which is within the range of the simulation, from -15 to 25°C . The physical properties were obtained from REFPROP version 7.0 [21]. The latent heat of CO₂ is higher than R236fa. The liquid to vapor density ratio of R236fa is much higher than that of CO₂. The liquid viscosity and the surface tension of R236fa are much higher than that of CO₂. The physical property differences may explain the different heat transfer and two-phase pressure drop behaviors for these two fluids in the simulations to be presented.

Figure 2 shows the variation of exit vapor quality x_e versus saturation temperature T_{sat} for R236fa and CO₂ at a mass flux $G = 1500$ kg/m²s and a base heat flux $q_b = 250$ W/cm² (2.5MW/m²) when they evaporate in the silicon multi-microchannel evaporator in Fig. 1. The local vapor quality x_z at position z along flow direction is determined according to energy balance as

$$x_z = \frac{z(W+t)q_b}{HWGi_{LV}} \quad (3)$$

The exit vapor quality x_e is thus obtained when z equals the micro-channel length L .

Both the selected mass flux and base heat flux here represent the maximum values used in the present study. It can be seen from Fig. 2 that the exit vapor qualities of CO₂ are much lower than those of R236fa at the same conditions. Furthermore, CO₂ has much lower liquid vapor density ratio, liquid/vapour viscosity ratio and liquid surface tension than R236fa. These are very meaningful when selecting a coolant for cooling microprocessors using the silicon multi microchannel evaporator because the two-phase pressure drop is directly proportional to

exit vapor quality x_e and is also affected by the liquid/vapor density and viscosity ratios, and the liquid surface tension.

3. Simulation of Flow Boiling Heat Transfer and Two-Phase Pressure Drops of CO₂

The recent flow boiling heat transfer and two-phase pressure drop models for CO₂ of Cheng et al. [1, 2] are used to simulate the heat transfer and pressure drop behaviors of CO₂ in microchannels with diameters ranging from 0.44 to 1 mm. For non-circular channels, the equivalent diameter D_{eq} should be used in these models. Thus, the microchannels in Fig. 1, with an equivalent diameter $D_{eq} = 0.44$ mm, is included in the simulations below. It should be pointed out that these models are thus slightly extrapolated below its minimum diameter limit of 0.6 mm. However, the predicted heat transfer and pressure drop results still show some interesting parametric trends which are helpful in selecting heat transfer coefficients for the simulation of base temperatures of the silicon multi-microchannel evaporator in Fig. 1. No equations of our CO₂ methods are presented here but can be found in [1, 2]. The experimental results for R236fa together with their test conditions and methods can be found in [14].

3.1. Simulation Results of CO₂ Flow Boiling Heat Transfer

Figure 3(a) shows the effect of channel diameter on CO₂ heat transfer. The heat transfer coefficient increases with decreasing channel diameter. However, this variation is not so notable in the selected diameter range of micro-channels.

Figure 3(b) shows the effect of saturation temperature on CO₂ heat transfer. The heat transfer coefficient increases with increasing saturation temperature from 0 to 15°C. The saturation temperature has a significant effect on the heat transfer coefficient.

Figure 3(c) shows the effect of heat flux on CO₂ heat transfer. The heat transfer coefficient increases strongly with increasing heat flux.

Figure 3(d) shows the effect of mass flux on CO₂ heat transfer. The heat transfer coefficient increases with increasing mass flux, with the variation becoming larger at high vapor qualities. However, the increase of heat transfer coefficient is not so notable in actual percentage terms.

3.2. Simulation Results of Two-Phase Pressure Drops of CO₂

Figure 4(a) shows the effect of channel diameter on CO₂ two-phase frictional pressure drop for a mass flux $G = 1500 \text{ kg/m}^2\text{s}$ and a saturation temperature $T_{sat} = 0^\circ\text{C}$. The two-phase frictional pressure drop increases with decreasing tube diameter and the diameter effect is significant. It should be pointed out that the minor inflections in the course at about vapor quality $x = 0.15$ are due to a change in flow pattern and hence in the pressure drop calculation. These minor inflections also appear in other figures for two-phase pressure drops.

Figure 4(b) shows the effect of saturation temperature on CO₂ two-phase pressure drop for a mass flux $G = 1500 \text{ kg/m}^2\text{s}$, a channel diameter $D = 0.44 \text{ mm}$ (equivalent diameter of the microchannels in Fig. 1 is used here and also in the whole paper) and a channel length $L = 20 \text{ mm}$. The two-phase frictional pressure drop decreases with saturation temperature. The effect of saturation temperature becomes significant at high vapor qualities.

Figure 4(c) shows the effect of mass flux on CO₂ two-phase frictional pressure drop for a channel diameter $D = 0.44 \text{ mm}$, a saturation temperature $T_{sat} = 0^\circ\text{C}$ and a channel length $L = 20 \text{ mm}$. The two-phase frictional pressure drop increases with mass flux.

The total two-phase pressure drop Δp_{total} for horizontal channel equals the two-phase frictional pressure drop Δp_f plus the acceleration pressure drop Δp_a as

$$\Delta p_{total} = \Delta p_f + \Delta p_a \quad (4)$$

$$\Delta p_a = G^2 \left\{ \left[\frac{(1-x)^2}{\rho_L(1-\varepsilon)} + \frac{x^2}{\rho_V \varepsilon} \right]_{out} - \left[\frac{(1-x)^2}{\rho_L(1-\varepsilon)} + \frac{x^2}{\rho_V \varepsilon} \right]_{in} \right\} \quad (5)$$

where void fraction ε is calculated with the Rouhani and Axelsson [22] correlation as

$$\varepsilon = \frac{x}{\rho_V} \left[(1+0.12(1-x)) \left(\frac{x}{\rho_V} + \frac{1-x}{\rho_L} \right) + \frac{1.18(1-x) [g\sigma(\rho_L - \rho_V)]^{1/4}}{G\rho_L^{1/2}} \right]^{-1} \quad (6)$$

It should be mentioned that the Rouhani and Axelsson void fraction correlation is used here for CO₂ because it is in consistence with the CO₂ flow pattern map, two-phase pressure drop and flow boiling heat transfer model [1, 2, 17, 18]. This correlation gives good void fraction prediction for CO₂ as in the CO₂ flow boiling heat transfer and two-phase pressure drop predictions [1, 2, 17, 18].

From the simulated pressure drop results, it may be concluded that a high saturation temperature and a low mass flux should be selected to obtain low pressure drops, so as to reduce the pumping power for a fixed channel diameter. In the case of a base heat flux $q_b = 250 \text{ W/cm}^2$ (2.5MW/m^2) which corresponds to an exit vapour quality of 0.5 for a mass flux $G = 1500 \text{ kg/m}^2\text{s}$ as indicated by the dashed line in Fig. 4(b), the frictional pressure

gradient is about 615 kPa/m. This corresponds to a frictional pressure drop less than 12.3 kPa for the microchannel length $L = 20$ mm. Considering the acceleration pressure drop Δp_a evaluated by Eq. (5), the total two-phase pressure drop Δp_{total} evaluated by Eq. (4) in a single microchannel is 16.3 kPa, which is much less than that for R236fa (162 kPa evaluated by the homogeneous model [14]). Thus, using CO₂ requires much less pumping power than R236fa for the same conditions.

4. Simulated Base Temperatures in a Multi-Microchannel Evaporator

Simulations of the base temperature of the silicon multi-microchannel evaporator in Fig. 1 were performed. First, wall heat fluxes q_w (it should be noted that a heat flux of 5 W/cm² was used here for those beyond this value due to the limitation of the heat transfer model) were assumed to predict the flow boiling heat transfer coefficients of CO₂ for certain conditions such as channel equivalent diameter, mass flux and saturation temperature. For the simplicity, no equations are given in this paper. The details of the flow boiling heat transfer model can be found in [1, 2]. One example of how to get heat transfer coefficient is indicated by the dashed line in Fig. 3(a), where the heat transfer coefficient is about 28.98 kW/m²K for the indicated condition. Then, Eq. (7) was used to determine the wall temperature T_w . Finally, Eqs. (8) to (12) were iteratively solved to obtain the base temperatures. The heat transfer coefficient was defined as

$$h = \frac{q_w}{T_w - T_{sat}} \quad (7)$$

and the base heat flux was evaluated as [23]:

$$q_b = q_w \frac{W + 2\eta H}{W + t} \quad (8)$$

where the fin efficiency was calculated as follows [23]:

$$\eta = \frac{\tanh(mH)}{mH} \quad (9)$$

$$m = \sqrt{\frac{h(W + L)}{k_{si}WL}} \quad (10)$$

The thermal conductivity of silicon was calculated as in [14]:

$$k_{si} = 0.0018T^2 - 0.7646T + 143.25 \quad (11)$$

The base temperature was calculated with a one dimensional heat conduct model as

$$T_b = T_w - \frac{q_b e}{k_{si}} \quad (12)$$

It should be pointed out here that the assumption of uniform heat flux is reasonable because the heating surface is very small and the two-phase pressure drop across the test section is 16.3 kPa which causes less than 0.2°C in saturation temperature decrease along the channel length of 20 mm. Furthermore, iteration method is used to calculate the base temperature considering the variable conductivity of silicon due to temperature effect. As shown in Fig. 3, the flow boiling heat transfer coefficient of CO₂ has slightly variation with local vapor quality (flat heat transfer coefficient curve), thus, the fin efficiency varies very slightly. In general, these effects on the simulated base temperatures are negligible. This also confirms the assumption of uniform heat flux assumption in the present study. Therefore, the averaged base temperatures are obtained in the simulations as shown in Figs. 5 to 7 because of the uniform distribution of heat fluxes on the very small surface area.

Figure 5 shows the simulated base temperatures of CO₂ flow boiling in the silicon multi-microchannel evaporator at three different saturation temperatures and a mass flux of 1000 kg/m²s. It can be seen that a lower saturation temperature can contribute to lower base temperatures. However, in practical applications, the higher energy cost caused by using a lower temperature should be considered.

Figure 6 shows the simulated base temperatures of CO₂ flow boiling in the silicon multi-microchannel evaporator at mass fluxes of 500 kg/m²s and 1500 kg/m²s and at a saturation temperature of 15°C. With the higher mass flux, a higher base heat flux may be cooled. For the lower mass flux, a more limited heat flux may be dissipated by the evaporator because of the limitation of the exit vapor quality x_e . For the lower mass flux at higher heat flux, the exit vapor quality may reach 1 and thus cooling is no longer effective.

Figure 7 shows the comparison of the simulated base temperatures of CO₂ and R236fa flow boiling in the silicon multi-microchannel evaporator at a mass flux of 987.6 kg/m²s and a saturation temperature of 25°C for base heat fluxes in the range from 20 to 100 W/cm². It can be seen that CO₂ can achieve lower base temperatures than R236fa by 4 to 6 K.

It should however be pointed out that very high heat flux cooling is beyond the applicable conditions of the CO₂ models. In the simulations, heat transfer coefficients at much lower heat fluxes (less than 5W/cm²) were used in the simulation. This makes the simulated results much more conservative. However, further experiments are needed for CO₂ flow boiling in microchannels to extend the heat transfer model to extremely high heat fluxes and to understand the physical mechanisms which might be quite different from those in macro- and mini-scale channels. Apparently, no such information is available so far.

Although CO₂ has much better thermal performance and much lower pumping power requirements than R236fa, it must be realized that the operational pressure of CO₂ is much higher than R236fa. Especially, no

experimental study on CO₂ evaporation in very tiny channels is available. Only some preliminary simulations are here presented in this study. Obviously, CO₂ also presents a great technological challenge like other new cooling technology. Therefore, efforts should be made to understand the fundamentals of CO₂ evaporation in micro-channels and to achieve the application of CO₂ flow boiling for chip cooling.

5. Conclusions

In this study, simulations of the base temperatures of a silicon multi-microchannel evaporator using CO₂ for evaporation were performed for base heat fluxes $q_b = 20-100 \text{ W/cm}^2$, a mass flux $G = 987.6 \text{ kg/m}^2\text{s}$ and a saturation temperature $T_{sat} = 25^\circ\text{C}$. It shows that the base temperatures using CO₂ are 4-6 K lower than those using R236fa. CO₂ has much higher heat transfer coefficients and lower two phase pressure drops in the multi-microchannel evaporator than R236fa. However, the operational pressure of CO₂ is much higher than that of R236fa. Based on the analysis and comparison, CO₂ appears to be a promising coolant for microprocessors for low temperature applications. Further study on the application of CO₂ flow boiling for chip cooling should be investigated.

Acknowledgement

The main contents of this paper were originally presented at the 6th International Conference on Heat Transfer, Fluid Mechanics and Thermodynamics, 30 June to 2 July, 2008, Pretoria, South Africa, with paper number CL2.

References

- [1] L. Cheng, G. Ribatski, J. Moreno Quibén, J.R. Thome, New prediction methods for CO₂ evaporation inside tubes: Part I-A two-phase flow pattern map and a flow pattern based phenomenological model for two-phase flow frictional pressure drops, *Int. J. Heat Mass transfer* 51 (2008) 111-124.

- [2] L. Cheng, G. Ribatski, J. Moreno Quibén, J.R. Thome, New prediction methods for CO₂ evaporation inside tubes: Part II-An updated general flow boiling heat transfer model based on flow patterns, *Int. J. Heat Mass transfer* 51 (2008) 125-135.
- [3] J.R. Thome, Recent advances in thermal modeling of micro-evaporators for cooling of microprocessors, ASME International Mechanical Engineering Congress and Exhibition (IMECE), Seattle, Nov. 10-16. 2007.
- [4] J.R. Thome, R. Revellin, B. Agostini, J.E. Park, Cooling of microprocessors using flow boiling of refrigerants in micro-evaporators, International Symposium on Phase Change, UK Heat Transfer 2007, Edinburgh, Scotland, Sept. 12. 2007.
- [5] L. Cheng, D. Mewes, A. Luke, Boiling phenomena with surfactants and polymeric additives: a state-of-the-art review, *Int. J. Heat Mass Transfer* 50 (2007) 2744-2771.
- [6] J.R. Thome, Boiling in microchannels: a review of experiment and theory, *Int. J. Heat Fluid Flow* 25 (2004) 128-139.
- [7] L. Cheng, D. Mewes, Review of two-phase flow and flow boiling of mixtures in small and mini channels, *Int. J. Multiphase Flow* 32 (2006) 183-207.
- [8] S.G. Kandlikar, Fundamental issues related to flow boiling in minichannels and microchannels, *Experimental Thermal Fluid Science* 26 (2002) 389-407
- [9] L. Cheng, G. Ribatski, J.R. Thome, Gas-liquid two-phase flow patterns and flow pattern maps: fundamentals and applications. *ASME Applied Mechanics Reviews* 61 (2008) 050802-1-050802-28.
- [10] D.B. Tuckerman, R.F.W. Pease, High performance heat-sinking for VLSI, *IEEE Electron Device Lett.* 2 (1981) 126-129.
- [11] G. Hetsroni, A. Mosyak, Z. Segal, Z., G. Ziskind, A uniform temperature heat sink for cooling of electronic devices, *Int. J. Heat Mass Transfer* 45 (2002) 3275-3286.
- [12] J. Lee, I. Mudawar, Two-phase flow in high-heat-flux micro-channel heat sink for refrigeration cooling applications: part I-pressure drop characteristics, *Int. J. Heat Mass Transfer* 48 (2005) 928-940.
- [13] J. Lee, I. Mudawar, Two-phase flow in high-heat-flux micro-channel heat sink for refrigeration cooling applications: part II-heat transfer characteristics, *Int. J. Heat Mass Transfer* 48 (2005) 941-955.
- [14] B. Agostini, J.R. Thome, M. Fabbri, D. Calmi, U. Kloter, B. Michel, High heat flux flow boiling in silicon multi-microchannels: Part I – heat transfer characteristics of R-236fa, *Int. J. Heat Mass Transfer* 51 (2008) 5400-5414.

- [15] B. Agostini, J.R. Thome, M. Fabbri, D. Calmi, U. Kloter, B. Michel, High heat flux flow boiling in silicon multi-microchannels: Part II – heat transfer characteristics of R-245fa, *Int. J. Heat Mass Transfer* 51 (2008) 5415-5425.
- [16] J.R. Thome, G. Ribatski, State-of-the art of flow boiling and two-phase flow of CO₂ in macro- and micro-channels, *Int. J. Refrigeration* 28 (2006) 1149-1168.
- [17] L. Cheng, G. Ribatski, L. Wojtan, J.R. Thome, New flow boiling heat transfer model and flow pattern map for carbon dioxide evaporating inside tubes, *Int. J. Heat Mass Transfer* 49 (2006) 4082-4094.
- [18] L. Cheng, G. Ribatski, L. Wojtan, J.R. Thome, Erratum to: New flow boiling heat transfer model and flow pattern map for carbon dioxide evaporating inside tubes, [*Heat Mass Transfer* 49 (21-22) (2006) 4082-4094], *Int. J. Heat Mass Transfer* 50 (2007) 391.
- [19] M.H. Kim, J. Pettersen, C.W. Bullard, Fundamental process and system design issues in CO₂ vapor compression systems, *Progr. Energ. Combust. Sci.* 30 (2004) 119-174.
- [20] L. Cheng, G. Ribatski, J.R. Thome, Analysis of supercritical CO₂ cooling in macro- and micro channels, *In. J. Refrigeration* 31 (2008) 1301-1316.
- [21] REFPROP. NIST Refrigerant Properties Database 23, Gaithersburg, MD, 2002, Version 7.0.
- [22] Z. Rouhani, E. Axelsson, Calculation of volume void fraction in a subcooled and quality region, *Int. J. Heat Mass Transfer* 17 (1970) 383-393.
- [23] F.P. Incropera, D.P. Dewitt, *Fundamental of Heat and Mass Transfer*, 5th ed., Wiley, New York, 2002.

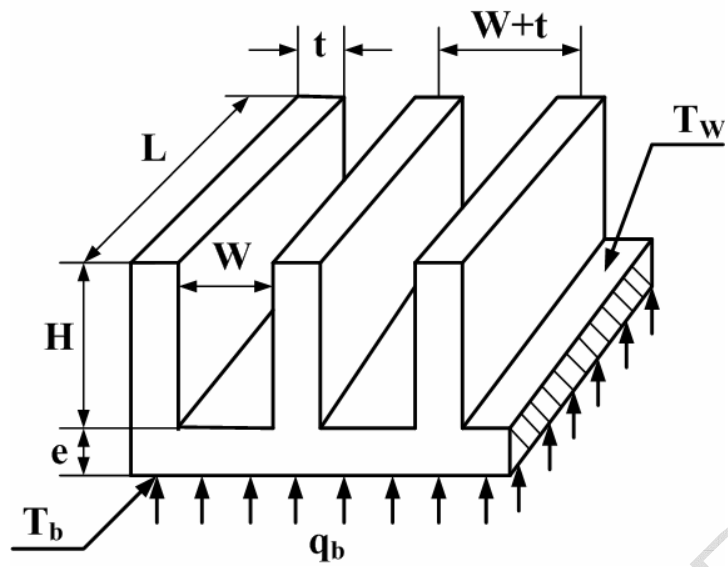


Figure 1 Schematic diagram of a silicon multi-microchannel evaporator used for chips cooling.

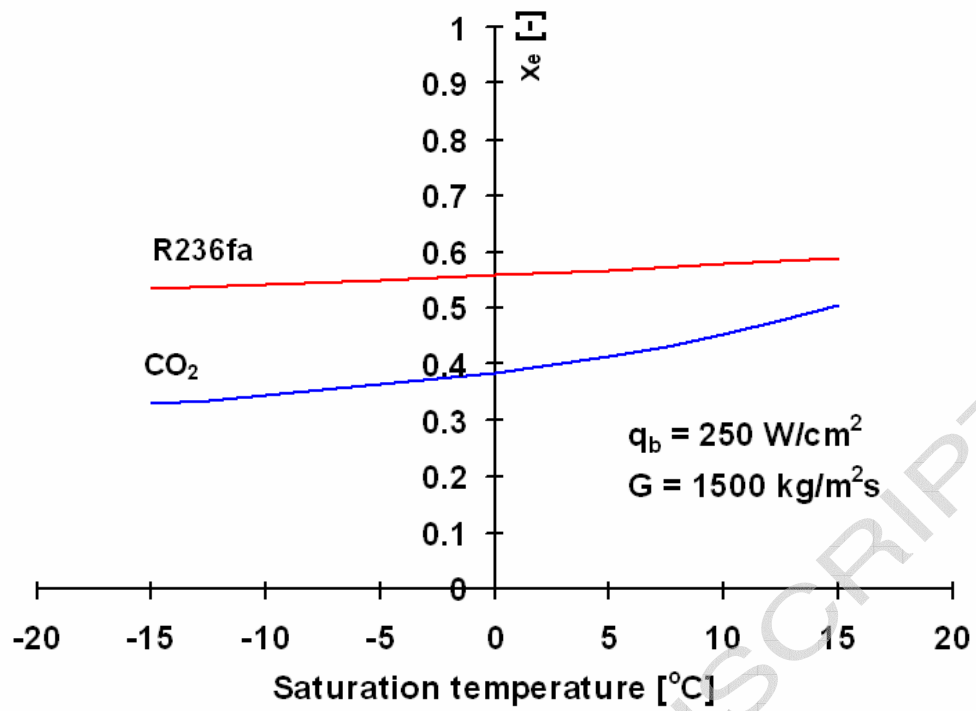
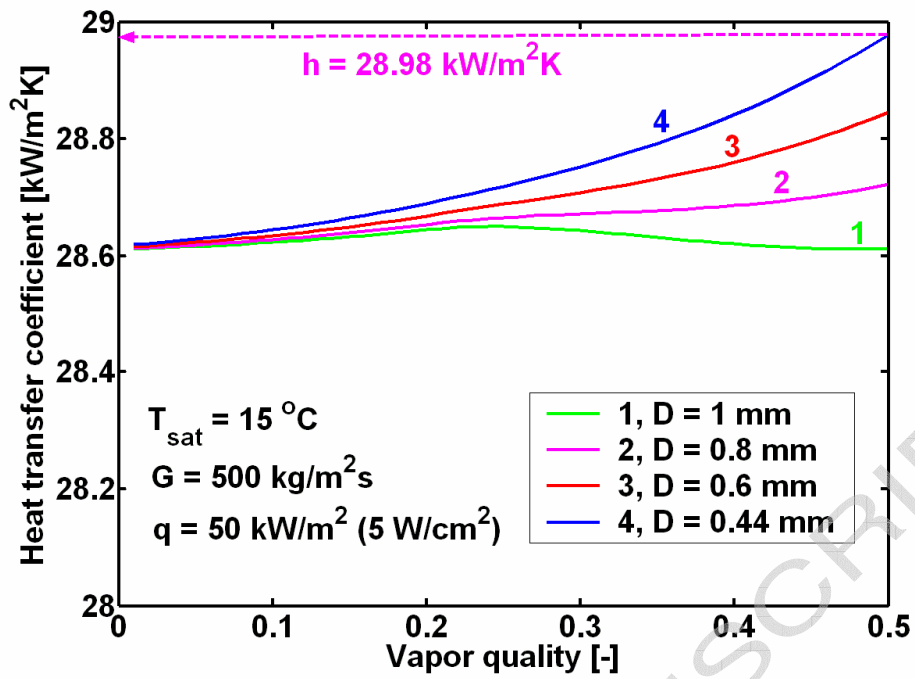
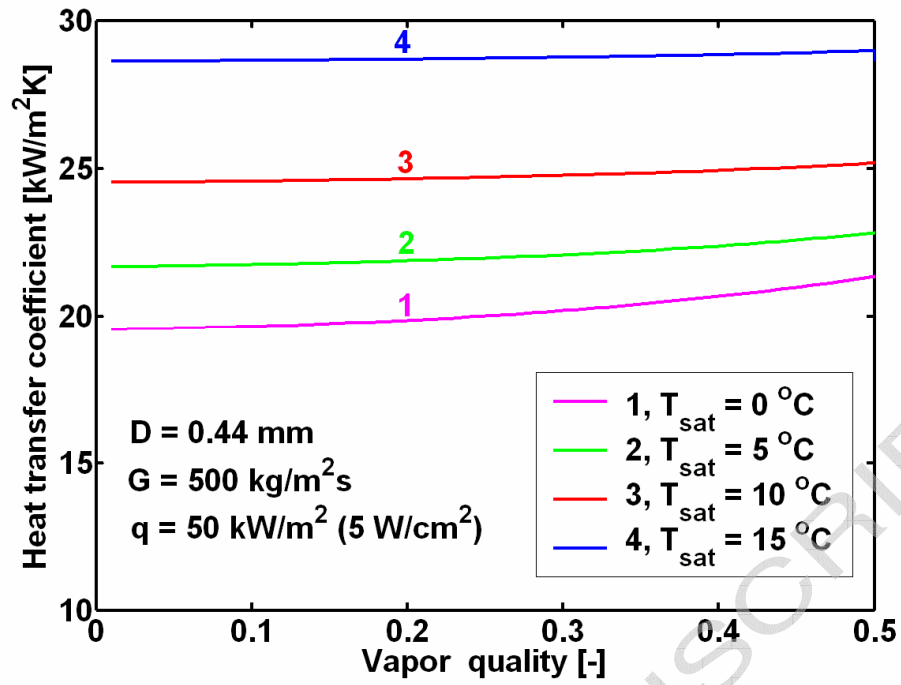


Figure 2 Exit vapor quality x_e versus saturation temperature T_{sat} for R236fa and CO_2 at the indicated conditions.



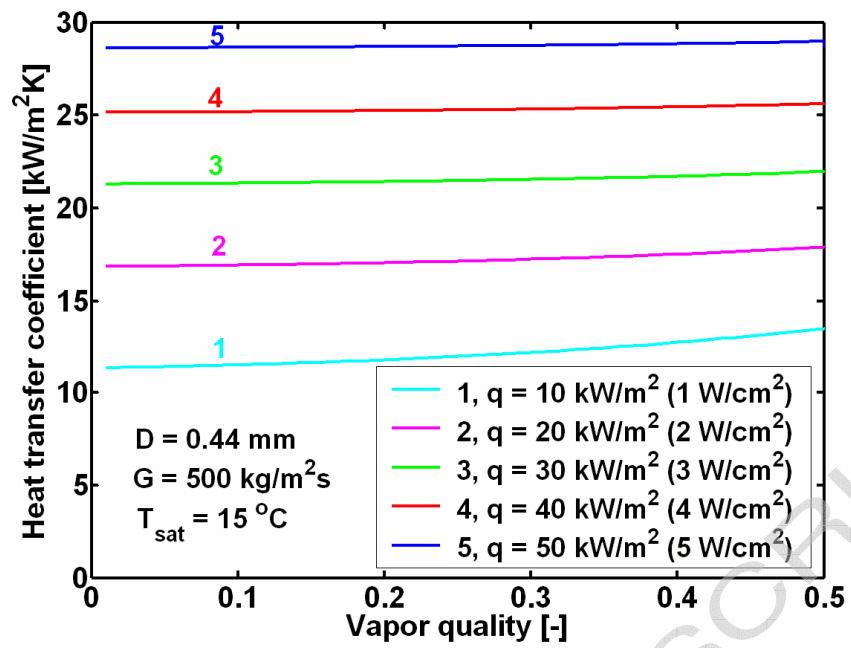
(a)

Figure 3 Simulation of flow boiling heat transfer of CO₂: (a) The effect of channel diameter;



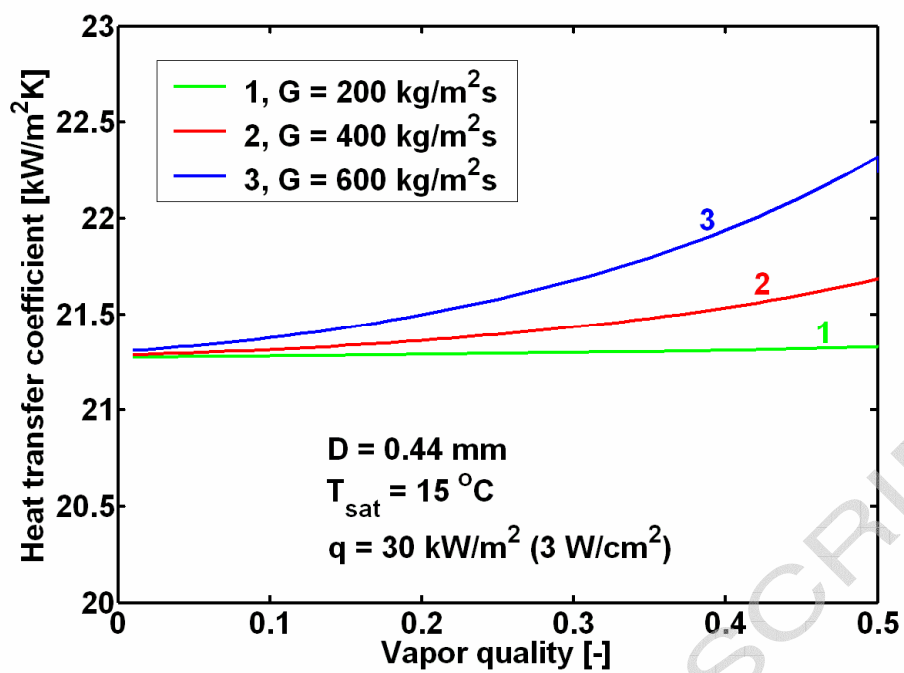
(b)

Figure 3 Simulation of flow boiling heat transfer of CO₂: (b) The effect of saturation temperature;



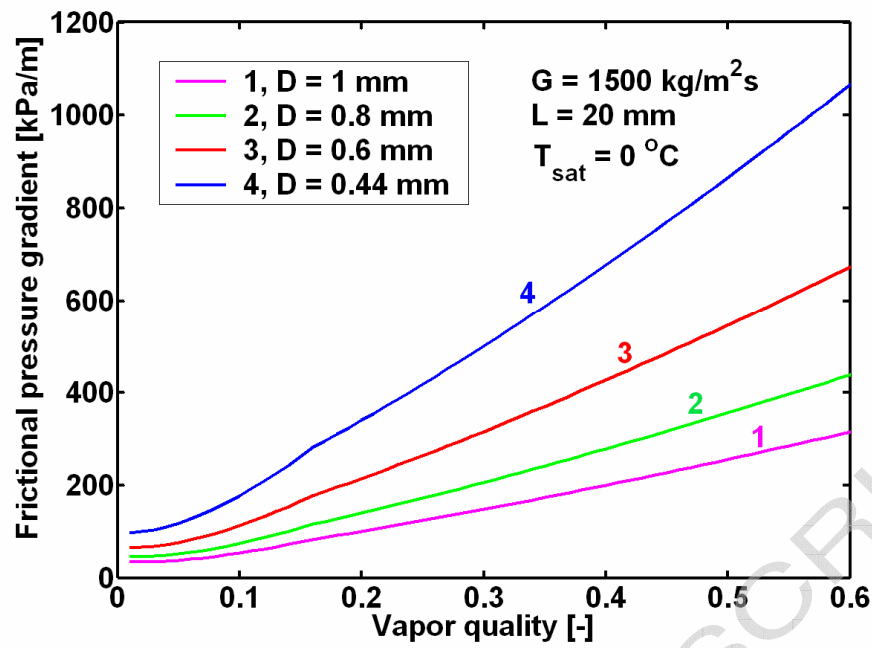
(c)

Figure 3 Simulation of flow boiling heat transfer of CO₂: (c) The effect of heat flux;



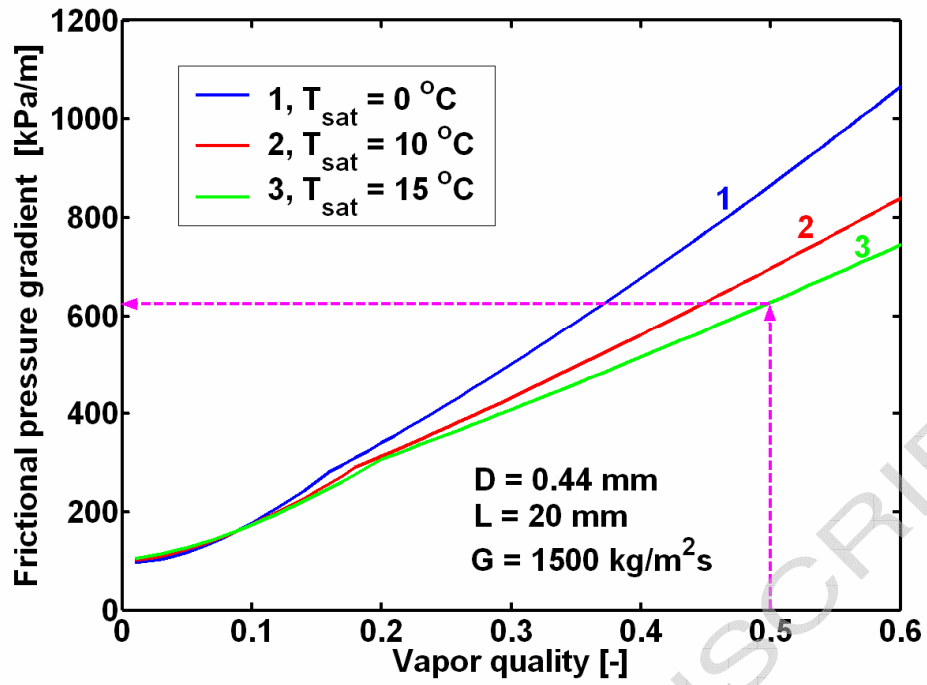
(d)

Figure 3 Simulation of flow boiling heat transfer of CO₂: (d) The effect of mass flux.



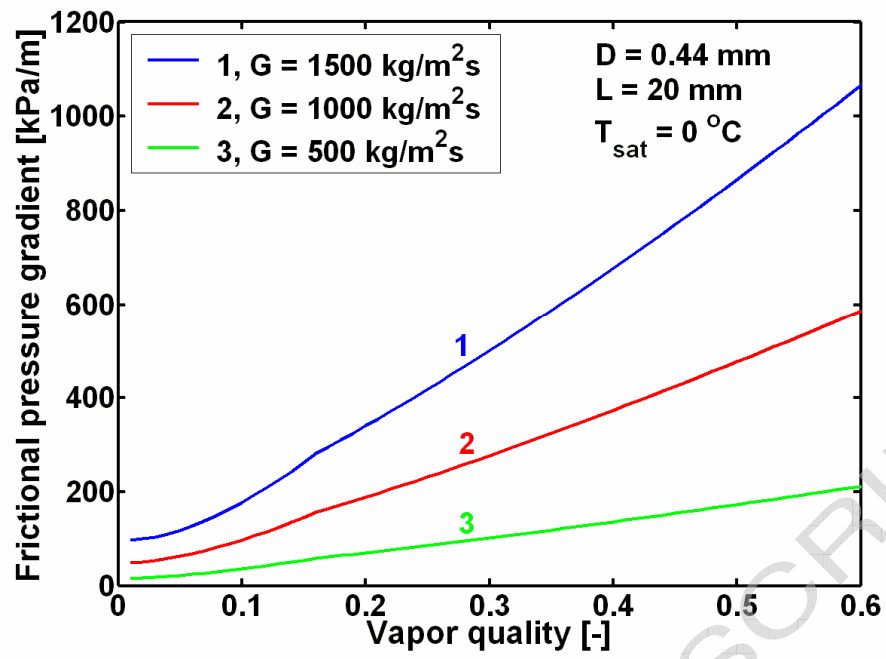
(a)

Figure 4 Simulation results of two-phase frictional pressure drops of CO₂: (a) The effect of channel diameter;



(b)

Figure 4 Simulation results of two-phase frictional pressure drops of CO₂: (b) The effect of saturation temperature,



(c)

Figure 4 Simulation results of two-phase frictional pressure drops of CO₂: (c) The effect of mass flux.

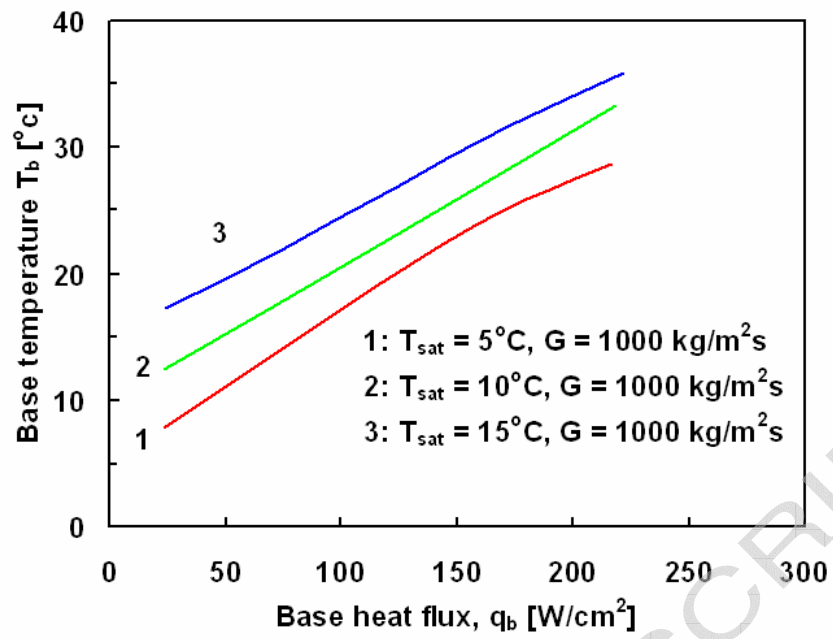


Figure 5 Simulation of base temperatures of CO₂ for different saturation temperatures at a fixed mass flux.

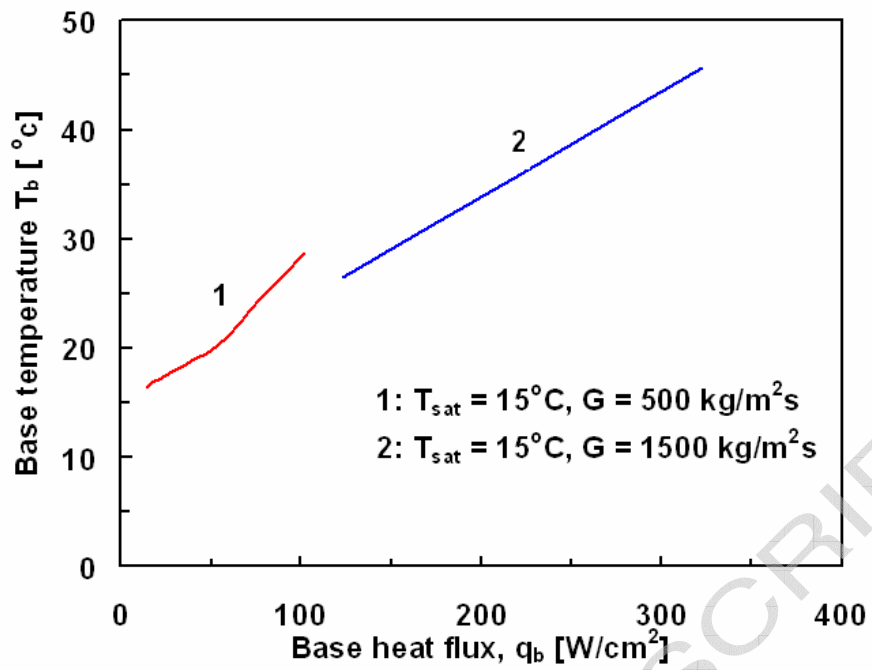


Figure 6 Simulation of base temperature of CO₂ for two different mass fluxes at a fixed saturation temperature.

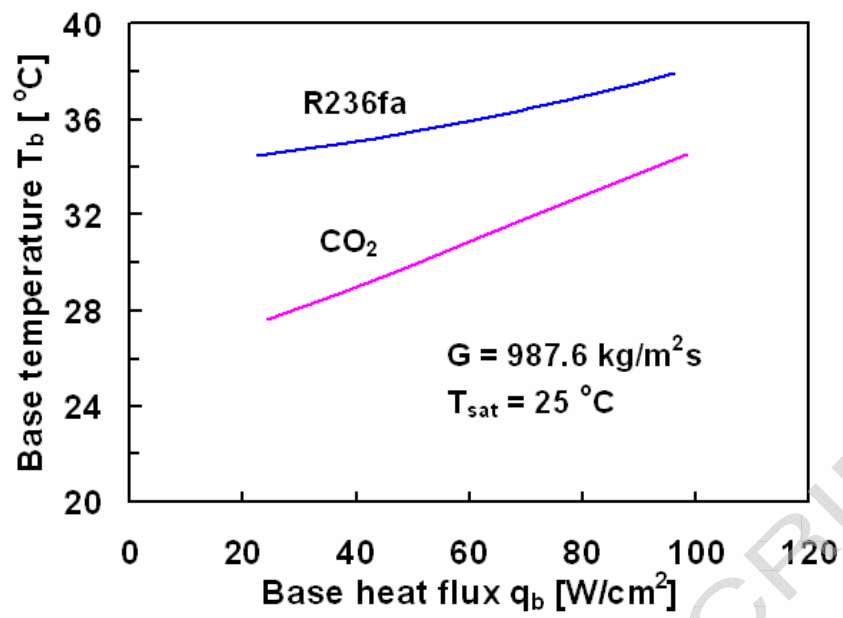


Figure 7 Comparisons of simulation results of base temperature of CO₂ and R236fa at the indicated conditions.

List of Figure Captions

Figure 1 Schematic diagram of a silicon multi-microchannel evaporator used for chips cooling.

Figure 2 Exit vapour quality x_e versus saturation temperature T_{sat} for R236fa and CO₂ at the indicated conditions.

Figure 3 Simulation of flow boiling heat transfer of CO₂: (a) The effect of channel diameter.

Figure 3 Simulation of flow boiling heat transfer of CO₂: (b) The effect of saturation temperature.

Figure 3 Simulation of flow boiling heat transfer of CO₂: (c) The effect of heat flux.

Figure 3 Simulation of flow boiling heat transfer of CO₂: (d) The effect of mass flux.

Figure 4 Simulation results of two-phase frictional pressure drops of CO₂: (a) The effect of channel diameter;

Figure 4 Simulation results of two-phase frictional pressure drops of CO₂: (b) The effect of saturation temperature;

Figure 4 Simulation results of two-phase frictional pressure drops of CO₂: (c) The effect of mass flux.

Figure 5 Simulation of base temperatures of CO₂ for different saturation temperatures at a fixed mass flux.

Figure 6 Simulation of base temperature of CO₂ for two different mass fluxes at a fixed saturation temperature.

Figure 7 Comparisons of simulation results of base temperature of CO₂ and R236fa at the indicated conditions.

Table 1 Channel dimensions.

L (mm)	H (mm)	W (mm)	t (mm)	e (mm)	N	D (mm)
20	0.68	0.223	0.08	0.32	67	0.336* 0.44**

* hydraulic diameter and **equivalent diameter.

ACCEPTED MANUSCRIPT

Table 2 Physical properties of R236fa and CO₂.

Physical properties	R236fa	CO ₂
T_{sat} (°C)	15	15
p_{sat} (MPa)	0.19	5.1
ρ_L (kg/m ³)	1392.8	821.2
ρ_V (kg/m ³)	13.1	160.7
i_{LV} (kJ/kg)	151.6	176.7
μ_L (μPas)	324.3	74.4
μ_V (μPas)	10.5	16.95
σ (N/m)	0.01125	0.00195

ACCEPTED MANUSCRIPT